Effect of Fiber Configuration on the Fiber-to-Mortar Bond Behavior

Ali Dalalbashi[1, a *], Bahman Ghiassi[2, b] and Daniel V. Oliveira[1, c]

[1]University of Minho, Department of Civil Engineering, ISISE

Guimarães, Portugal

[2]Centre for Structural Engineering and Informatics, Faculty of Engineering, University of Nottingham

Nottingham, United Kingdom

[a]alidalalbashi@gmail.com, [b]bahman.ghiassi@nottingham.ac.uk, [c]danvco@civil.uminho.pt

Keywords: Fiber/matrix bond; Pull-out testing; Mechanical testing.

Abstract. Textile-reinforced mortar (*TRM*) composites have received extensive attention as a sustainable solution for seismic strengthening of masonry and historical structures. This new system is composed of textile fibers embedded in an inorganic matrix and is applied on the masonry substrate surface as an externally bonded reinforcement (*EBR*) system. The bond at the textile-to-mortar and at the mortar-to-substrate interfaces are the main stress-transfer mechanisms and therefore should be thoroughly investigated.

Although several studies have been focused on characterization of the bond behavior in *TRM*-masonry composites during the last years, there is still a lack of suitable constitutive laws. Most of the available studies have addressed the bond behavior through single-lap shear bond tests in which the bond of the TRM system to masonry substrate is evaluated. The bond performance between the fiber and mortar, however, has received few attention and is the main subject of this study.

The presented work consist of fiber pull-out tests on a (unidirectional) steel-based and a (bidirectional) glass-based *TRM* composite as common reinforcing systems. The roles of transverse fibers (in glass-based TRM) as well as number of fibers on the bond behavior are also investigated. The results show that transverse elements cause toughness to increase. In addition, by increasing the number of fibers, the obtained failure modes change from slipping to mortar cracking.

Introduction

The advantages of textile reinforced mortar (*TRM*) composites to fiber reinforced polymers (*FRPs*) like the fire resistance, the vapor permeability, the removability, and the compatibility with masonry and concrete substrates [1–3] have made these composites very interesting for externally bonded reinforcement of masonry and reinforced concrete structures.

TRMs composed of continues fibers embedded in a matrix are used with a variety of unidirectional and bidirectional fibers and mortar types, which makes development of unified design relations for these materials a complicated task. Glass, steel and basalt are among the most common fiber types used. While for the matrix, cementitious or lime-based mortars are usually used. Lime-based mortars are preferred for application to masonry and historical structures due to compatibility, sustainability issues, breathability and capability of accommodating structural movements [4–6].

While most of the attention by the scientific community have been given to the tensile response of *TRMs* and to the *TRM*-to-substrate bond behavior, the fiber-to-mortar bond response is relatively unknown and poorly addressed [7–10].

In this study, an experimental campaign is carried out on the effect of fiber configuration (like number of fibers and presence of transverse fibers) on the bond response of textile-to-mortar. For this purpose, a series of pull-out tests are conducted based on unidirectional steel and bidirectional glass fibers as well as two commercially available hydraulic lime mortars.

Experimental Tests

Material Characterization Tests. Two commercially available hydraulic lime-based mortars as the matrix referred as *M1* and *M2* are used throughout this paper. Mortar *M1* is a high-ductility hydraulic lime mortar and mortar *M2* is a pure natural hydraulic lime with mineral geo-binder base. For mechanical characterization of the mortar, compressive and flexural tests are performed according to *ASTM C*109 [11] and *EN* 1015-11 [12] at different ages (3, 7, 14, 28, 60, 90 days). Five cubic (50×50×50 mm^3) and five prismatic (40×40×160 mm^3) specimens are prepared for compressive and flexural tests at each age, respectively.

The reinforcing materials are glass and steel fibers. The glass fiber is a woven biaxial fabric mesh made of an alkali-resistance fiberglass. Its mesh size and load resistance area per unit of width are equal to 25×25 mm^2 and 35.27 mm^2/ m, respectively. The steel fiber is a unidirectional ultra-high tensile steel sheet, with a density of 670 g/m^2, an effective area of one cord (five wires) equal to 0.538 mm^2. Direct tensile tests are performed on fibers to obtain their tensile strength and elastic modulus. A universal testing machine with a maximum load capacity of 10 kN and the rate of 0.3 mm/min is used for these tests. In this paper, the mortar-fiber pairs are taken from the same manufacturer meaning that glass fibers are used with mortar *M1* and steel fibers with mortar *M2*.

Pull-out Test. The single-sided pull-out test setup developed and presented by the authors in [13] is used in this study for investigating the fiber-to-mortar bond performance. The specimens consist of fibers embedded in disk shaped mortars with a thickness of 16 mm (see Fig. 1). The free length of the fiber is embedded in an epoxy resin block with a rectangular cross-sectional area of 10×16 mm^2, as shown in Fig. 1. For detailed information on the procedure followed for preparation of the specimens the reader is referred to [13]. The specimens are demolded after 24 hours of preparation and are placed in a damp environment for seven days. After that, the specimens are stored in the lab environmental conditions (20°C, 60% RH) until the test day (At the age of 60 days).

For investigating the effect of fiber configuration, three cases are considered for each material type, as shown in Fig. 1. For the glass-based *TRMs*, these cases include embedment of *single fiber*, *single fiber + transverse elements*, and *group of fibers* with a 50 mm embedment length (Fig. 1a-c). For the steel-based *TRMs*, since a unidirectional steel fiber mesh is used in this study, the specimens are prepared with embedment of *one single fiber*, *two fibers*, and *four fibers* in the mortar with a 150 mm embedment length (see Fig. 1d-f).

The specimens are named as *vv-wxy*, hereafter, in which *vv* is related to the mortar type (*M1* and *M2*). *w* is connected to the fiber type (*S*: steel and *S*: glass). *x* is linked to the fiber configuration (*S*: single, *T*: single+ transverse, *G*: group) and *y* is the number of fibers as illustrated in Table 1. For example, specimen *M2-SG4* is the specimen made with a four steel fibers embedded in mortar *M2*.

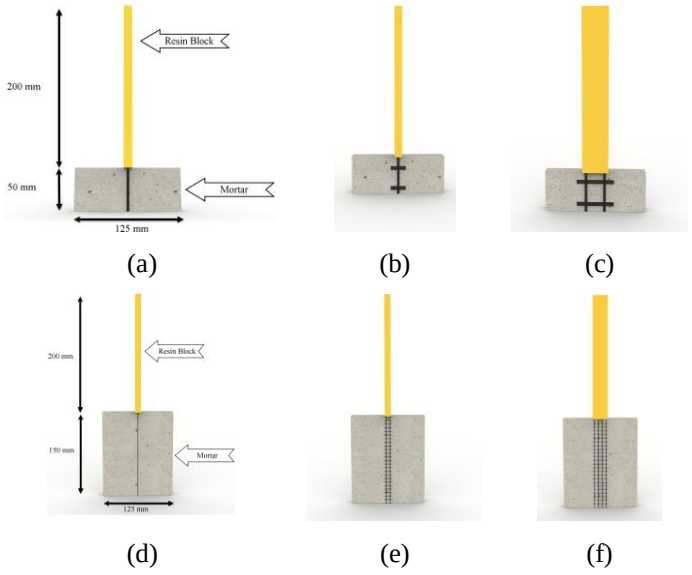

Fig. 1: Details of specimens for investigating the effect of fiber configuration on bond properties: (a) M1-GS1; (b) M1-GT1; (c) M1-GG2; (d) M2-SS1; (e) M2-SG2; (f) M2-SG4.

Table 1: Nomenclature for test specimens.

Mortar	Fiber	Fiber configuration	Name of specimens
M1	glass	single fiber	M1-GS1
		single fiber + transverse	M1-GT1
		group (2 fibers)	M1-GG2
M2	steel	single fiber	M2-SS1
		group (2 fibers)	M2-SG2
		group (4 fibers)	M2-SG4

For performing the tests, a u-shape steel support is used for supporting the specimens to a rigid frame. A mechanical clamp is used to grip the epoxy resin (and thus the fiber) from the top and performing the tests (Fig. 2). Two *LVDTs* with 20 mm range and 2-µm sensibility are located at both sides of the epoxy block to record the slip. The average of these *LVDT* measurements is presented as the slip in the experimental results. All the tests are carried out using a servo-hydraulic system with a maximum capacity of 25 kN at a displacement rate of 1.0 mm/min.

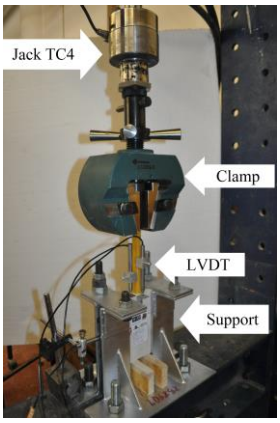

Fig. 2: Pull-out test setup.

Results and discussion

Material Properties. The mean compressive and flexural strength of the mortar at different ages are presented in Table 2. As illustrated, the strength of both mortars increase significantly during the first 30 days and, besides some variations, the changes (particularly for the compressive strength) are not significant after that.

Table 2: Mortar mechanical properties.*

Mortar	Test	3 days	7 days	14 days	28 days	60 days	90 days
M1	compressive strength [mpa]	0.91 (4.5)	3.77 (5.4)	5.91 (9.2)	7.07 (10.5)	8.31 (12.2)	7.84 (4.7)
	flexural strenght [mpa]	-	2.51 (8.1)	4.03 (3.6)	4.71 (7.8)	5.10 (3.2)	4.66 (8.9)
M2	compressive strength [mpa]	3.88 (8.5)	6.46 (7.8)	8.76 (7.8)	9.53 (11.1)	8.81 (13.8)	8.89 (5.9)
	flexural strenght [mpa]	1.4 (3.3)	1.53 (4.0)	1.79 (13.5)	2.54 (9.6)	2.09 (8.3)	2.33 (10.6)

*CoV of the results are given in percentage inside parentheses.

The envelope and average tensile stress-strain curves obtained from direct tensile tests on dry fibers are also shown in Fig. 3. The results show an average tensile strength, Young's modulus, and rupture strain of the steel fiber are 2972 MPa, 189.34 GPa, and 1.88 %, respectively (Fig. 3a). These values are equal to 875 MPa, 65.94 GPa, and 1.77 %, respectively, for the glass fiber (Fig. 3b).

Textile-to-Mortar Bond Response. The main outcomes of the pull-out tests that are used for investigation of the bond behavior and can significantly affect the experimental interpretations are the peak load, the initial stiffness, and consequently the toughness [14]. In the following paragraphs, the bond response of different fiber configurations and the failure modes will be investigated.

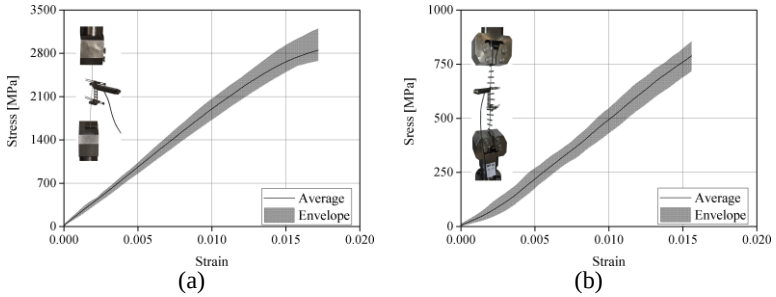

Fig. 3: Tensile stress-strain curves for: (a) steel fiber; (b) glass fiber.

Steel Reinforced Mortar. The average and envelop of the load-slip curves obtained from steel-based *TRMs* with different configurations are shown in Fig. 4. The results are presented in terms of the applied load per fiber (load divided by the number of fibers) versus slip to facilitate comparison between different configurations.

It can be observed that although the steel fibers are unidirectional, the pull-out response of single fibers is different than that of the group of fibers. The failure mode of the specimens, as shown in Fig. 5, also changes from fiber slippage in single fiber specimens to mortar cracking and splitting in the group fiber specimens. The pull-out curve of the single fiber specimens (M2-SS1, Fig. 4a) shows a second peak load followed by a load reduction after complete debonding. This second peak load is not observed in the group fiber specimens (M2-SG2 and M2-SG4), Fig. 4b, c. which can be due to occurrence of mortar cracking and splitting after the peak load. From the presented curves, it can be observed that in contrast to the single fiber specimens (M2-SS1, Fig. 4a), the slip measurements are different from that of internal *LVDT* measurements in the group fiber specimens. This, although does not affect the obtained results, shows that by increasing the number of fibers the deformation of the resin block used for gripping the specimens becomes significant leading to a large difference between these two measurements.

A comparison between the average pull-out response in different configurations, illustrated in Table 3, clearly shows that by increasing the number of fibers the debonding load, the slip corresponding to the peak load, the toughness and initial stiffness of the load-slip curves decrease.

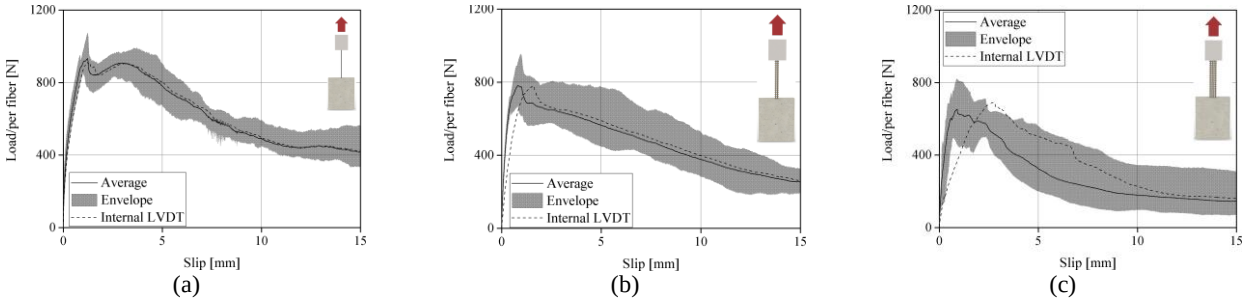

Fig. 4: Pull-out response of steel-based *TRMs* with different configurations: (a) M2-SS1; (b) M2-SG2; (c) M2-SG4.

Fig. 5: Failure modes of steel-based *TRMs* with different configurations: (a) M2-SS1; (b) M2-SG2; (c) M2-SG4.

Glass Reinforced Mortar. The average and envelop of the pull-out curves obtained from the glass-based *TRMs* with different configurations are shown in Fig. 6. The difference between the single-fiber and group fiber specimens is more significant in this case, which can be attributed to the effect of transverse elements. The main parameters of the pull-out curves are also summarized in Table 3.

Table 3. Changes of bond properties in steel-based and glass-based *TRM* with different fiber configurations.*

Fiber	Specimen	Slip corresponding to peak load [mm]	Peak load/ per fiber [N]	Toughness until peak load/ per fiber [N.mm]	Initial stiffness/ per fiber [N/mm]
steel	M2SS1	1.08 (17.6)	992 (9.8)	730 (23.2)	2772 (18.2)
	M2SG2	0.89 (26)	815 (14.2)	538 (29.8)	2863 (30.3)
	M2SG4	0.74 (43.8)	700 (15)	340 (57.1)	2058 (61.6)
glass	M1GS1	1.92 (24.6)	335 (6.9)	522 (23.9)	1588 (47.5)
	M1GT1	2.93 (17.5)	367 (7.6)	773 (26.9)	795 (29.5)
	M1GG2	7.05 (17.8)	404 (8.1)	2311 (17.1)	1238 (28.2)

*CoV of the results are given in percentage inside parentheses.

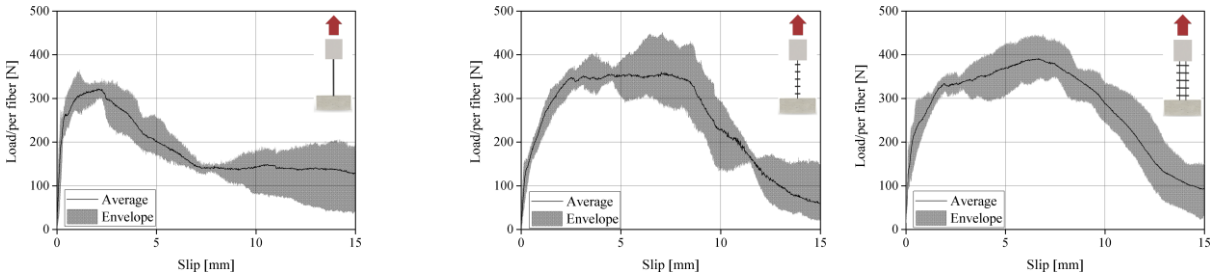

Fig. 6: Pull-out response of glass-based *TRMs* with different configurations: (a) M1-GS1; (b) M1-GT1; (c) M1-GG2.

In general, the specimens made of *single* fibers (M1-GS1 specimens) show all the three conventional stages of the pull-out behavior (elastic part, nonlinear part, dynamic part), see Fig. 6a [13–16]. On the other hand, the specimens made of *single+ transverse* (M1-GT1) and the group specimens (M1-GG2) do not have the typical drop of the pull-out load after the peak (Fig. 6b, c). In contrary, the pull-out curves in these specimens show a slip hardening behavior and a pseudo ductility before the final load drop. This strain hardening behavior can be attributed to the contribution of the transverse fibers to the bond response. It should also be reported that the fibers slippage in M1-GT1 and M1-GG2 specimens is followed by breakage of the transverse fibers at the last stage of the tests.

Conclusion

A comprehensive experimental investigation with the aim of characterizing the textile-to-mortar bond response in *TRM* composites was presented in this study. The effect of number of longitudinal fibers and transverse fibers on the bond behavior was examined. In general, it was observed:

- By increasing the number of steel fibers in pull-out tests, the failure mode changed from pull-out (for single fiber) to pull-out and mortar cracking (for group fibers).
- The transverse fibers had a significant influence on the bond behavior in glass-based *TRM* used in the current study. The toughness increased dramatically in the specimens containing transverse elements.

Acknowledgements

This work was partly financed by FEDER funds through the Operational Programme Competitiveness Factors (COMPETE 2020) and by national funds through the Foundation for Science and Technology (FCT) within the scope of project POCI-01-0145-FEDER-007633. The support to the first author through the grant SFRH/BD/131282/2017 is acknowledged.

References

[1] Carozzi FG, Poggi C. Mechanical properties and debonding strength of Fabric Reinforced Cementitious Matrix (FRCM) systems for masonry strengthening. Compos Part B Eng 2015;70:215–30. doi:10.1016/j.compositesb.2014.10.056.

[2] Razavizadeh A, Ghiassi B, Oliveira D V. Bond behavior of SRG-strengthened masonry

units: Testing and numerical modeling. Constr Build Mater 2014;64:387–97. doi:10.1016/j.conbuildmat.2014.04.070.

[3] Papanicolaou CG, Triantafillou TC, Papathanasiou M, Karlos K. Textile-reinforced mortar (TRM) versus FRP as strengthening material of URM walls: in-plane cyclic loading. Mater Struct 2007;40:1081–97. doi:10.1617/s11527-006-9207-8.

[4] Barr S, Mccarter WJ, Suryanto B. Bond-strength performance of hydraulic lime and natural cement mortared sandstone masonry. Constr Build Mater 2015;84:128–35. doi:10.1016/j.conbuildmat.2015.03.016.

[5] Pavlík V, Uzáková M. Effect of curing conditions on the properties of lime, lime–metakaolin and lime–zeolite mortars. Constr Build Mater 2016;102:14–25. doi:10.1016/j.conbuildmat.2015.10.128.

[6] Lanas J, Perez Bernal JL, Bello MA, Alvarez JI. Mechanical properties of masonry repair dolomitic lime-based mortars. Cem Concr Res 2006;36:951–60. doi:10.1016/j.cemconres.2005.10.004.

[7] Lignola GP, Caggegi C, Ceroni F, De Santis S, Krajewski P, Lourenço PB, et al. Performance assessment of basalt FRCM for retrofit applications on masonry. Compos Part B Eng 2017;128:1–18. doi:10.1016/j.compositesb.2017.05.003.

[8] Yu J, Yao J, Lin X, Li H, Lam JYK, Leung CKY, et al. Tensile performance of sustainable Strain-Hardening Cementitious Composites with hybrid PVA and recycled PET fibers. Cem Concr Res 2018;107:110–23. doi:10.1016/j.cemconres.2018.02.013.

[9] Leone M, Aiello MA, Balsamo A, Carozzi FG, Ceroni F, Corradi M, et al. Glass fabric reinforced cementitious matrix: Tensile properties and bond performance on masonry substrate. Compos Part B Eng 2017;127. doi:10.1016/j.compositesb.2017.06.028.

[10] Ghiassi B, Oliveira D V, Marques V, Soares E, Maljaee H. Multi-level characterization of steel reinforced mortars for strengthening of masonry structures. Mater Des 2016;110:903–13. doi:10.1016/j.matdes.2016.08.034.

[11] ASTM C109/C109M-05, Standard test method for compressive strength of hydraulic cement mortars (Using 2-in. or [50-mm] Cube Specimens). vol. 04. 2005. doi:10.1520/C0109_C0109M-05.

[12] BS EN 1015-11, Methods of test for mortar for masonry. Determination of flexural and compressive strength of hardened mortar. 1999.

[13] Dalalbashi A, Ghiassi B, Oliveira DV, Freitas A. Effect of test setup on the fiber-to-mortar pullout response in TRM composites: experimental and analytical modeling. Compos Part B Eng 2018;143:250–68. doi:10.1016/j.compositesb.2018.02.010.

[14] Mobasher B. Mechanics of Fiber and Textile Reinforced Cement Composites. London- New York: Taylor & Francis Group; 2012.

[15] Naaman AE, Namur GG, Alwan JM, Najm HS. Fiber pullout and bond slip. i: analytical study. J Struct Eng 1991;117:2769–90. doi:10.1061/(ASCE)0733-9445(1991)117:9(2769).

[16] Maljaee H, Ghiassi B, Lourenço PB, Oliveira D V. Moisture-induced degradation of interfacial bond in FRP-strengthened masonry. Compos Part B 2016;87:47–58. doi:10.1016/j.compositesb.2015.10.022.